의학박사 학위논문

An endogenous VEGF inhibitor, KAI1, is a master switch of angiogenesis

내재적 VEGF 억제자인 KAI1 의 혈관신생 조절에 관한 연구

2018 년 08 월

서울대학교 대학원

의과학과 의과학전공

최 재 일

A thesis of the Degree of Doctor of Philosophy

내재적 VEGF 억제자인 KAI1 의 혈관신생 조절에 관한 연구

An endogenous VEGF inhibitor, KAI1, is a master switch of angiogenesis

August 2018

The Department of Biomedical Sciences

Seoul National University

College of Medicine

Jae Il Choi

ABSTRACT

Angiogenesis represents new blood-vessel formation controlled by numerous factors. VEGF, the most potent pro-angiogenic factor, is commonly targeted in cancer therapy. However, little is known about endogenous VEGF inhibitors and their control. Here, CD82/KAI1 expressed on pericytes (PCs) acts as an endogenous anti-angiogenic factor. Through transcriptome and functional analysis, I revealed that leukemia inhibitory factor (LIF) is an anti-angiogenic effector molecule of KAI1 through KAI1-Src-p53 axis. Furthermore, KAI1 was shown to bind VEGF and PDGF-BB, preventing VEGFR/PDGFR signalling and tube formation by endothelial cells. In the therapeutic aspect, *KAI1*-overexpressing pericytes or recombinant KAI1 protein inhibited angiogenesis and cancer cell growth. Taken together, I demonstrated that KAI1 is a key regulator of angiogenesis by interacting with the angiogenic niche, and identified novel molecular mechanisms underlying anti-VEGF/PDGF therapy, which may help develop new anti-cancer strategies.

Keywords: KAI1, Angiogenesis, endogenous VEGF inhibitor, Perivascular cell

Student number: 2013-23535

CONTENTS

LIST OF TABLES AND FIGURES

LIST OF ABBREVIATIONS

ECs, Endothelial cells

PCs, Pericytes

VEGF, Vascular endothelial growth factor

FGF2, Basic fibroblast growth factor (basic fibroblast growth factor, bFGF)

PDGF-BB, Platelet-derived growth factor-BB

LIF, Leukemia inhibitory factor

GFP, Green fluorescent protein

RT-PCR, Reverse transcription polymerase chain reaction

PKC, Protein kinase C

SRC, Proto-oncogene tyrosine-protein kinase Src

An endogenous VEGF inhibitor, KAI1, is a master switch of angiogenesis

INTRODUCTION

Angiogenesis is a process of new blood vessel formation from the pre-existing vasculature, which is strictly controlled through a proper balance between pro- and anti-angiogenic factors[1]. This process is controlled by the interactions between two vascular cell types, endothelial cells (ECs) and pericytes. Although the role of the ECs in angiogenesis has been extensively studied, pericytes have only been shown to participate in vessel stabilization and paracrine signalling[1].

KAI1/CD82, a transmembrane protein and a member of the tetraspanin superfamily, is an evolutionally conserved molecule expressed in various tissue types. First identified as involved in the T-cell activation process, KAI1 has been primarily considered a suppressor of metastasis[2]. Recently, we and others reported that KAI1 regulates cell cycle progression of the long-term repopulating hematopoietic stem cells and muscle stem-progenitor cells[3,4].

To date, at least 27 endogenous inhibitors of angiogenesis have been identified and detected in blood[5]. Most of them originate from the fragments of large extracellular matrix and non-matrix derived-molecules, but the tetraspanin superfamily-derived endogenous inhibitors of angiogenesis have not been reported previously.

VEGF is the most potent angiogenesis initiator, and most of developing anti-angiogenic drugs for cancer therapy is focused on blocking VEGF or VEGFR signaling. Very extensive knowledge has been accumulated about mechanism of angiogenesis caused by VEGF[6], however, little is known about endogenous VEGF inhibitor, and their control mechanism of anti-angiogenic process.

Previously, I revealed KAI1 was shown to be expressed on the pericytes in the bone marrow stem cell niche. However, the role of KAI1-expressing pericytes in the regulation of angiogenesis remains unexplored, and here, determine its role in the angiogenesis and evaluate its potential to be used for cancer therapy.

MATERIALS AND METHODS

Mice

Adult C57BL/6 mice (6–12 weeks) were purchased from Jackson Laboratories. All animal experiments were approved by the Institutional Animal Care and Use Committee (IACUC) at Seoul National University Hospital (Approved number: SNU-160304-5-1) and complied with the National Research Council (NRC) 'Guidelines for the Care and Use of Laboratory Animals'. *Kai1* K/O mice were a generous gift from Professor Sung-Hee Baek at Seoul National University.

Generation of KAI1/CD82-emGFP fusion transgenic mouse

KAI1/CD82-EmGFP mouse was generated by Macrogen, Inc using CRISPR system and mice were interbred and maintained in pathogen-free condition at Macrogen, Inc (Seoul, Korea). All animal experiments were performed in accordance with the Korean Food and Drug Administration (KFDA) guidelines. Protocols were reviewed and approved by IACUC of Macrogen, Inc. All manipulations were conducted with the Institutional Animal Care and Use Committee approval (Approved number:

MS-2017-01).

Briefly, pregnant mare serum gonadotropin (PMSG), human chorionic gonadotropin (HCG) were treated into C57BL/6N female mice. After 48 hrs, these female mice were mated with C57BL/6N stud male mice. Next day, virginal plug checked female mice were sacrificed and harvested fertilized embryos. sgRNA3 and sgRNA4 and Cas9 nuclease and dsDonor were mixed and microinjected into one cell embryo. Microinjected embryos were incubated at 37° C during 1-2 hrs. Fourteen to sixteen injected one cell staged embryo were transplanted into oviducts of pseudopregnant recipient mice (ICR). After Founders were born, genotyping using tail cut samples was performed by PCR (F1: CCCTTGTTAGTCCCCTCCTC, R1: TTACTTGTACAGCTCGTCCA; R2: CCCACACCCCTAAGTTGTCA). PCR Positive samples were performed TA Cloning and analyzed by sequencing.

Mouse tumour graft model

For efficacy evaluation of rhKAI1 and supernatant of KAI1 overexpressed pericytes, $2x10^6$ PC-3 (human prostate cancer

cell line) cells and $2x10^6$ B16 (mouse melanoma cancer cell line) were mixed with rhKAI1 protein (4ug) or conditioned media of mock or *Kai1* O/E 10T1/2, and subsequently embedded in 100㎕ of Matrigel (Corning). NSG mice were subcutaneously injected with 100㎕ of Matrigel-cell mixture in the dorsal area. After 14 days, mice were sacrificed in order to harvest tumor tissues. The tissues were fixed with 4% paraformaldehyde (Wako), paraffin-embedded and mounted on slide glasses. Later, the samples were examined immunofluorescence analysis.

Cells

MS1 (mouse endothelial cell line) cells were cultured in DMEM high glucose (Gibco) supplemented with 10% FBS (Gibco) and 1X Antibiotics-antimycotics (Gibco). C3H/10T1/2 (mouse perivascular cell line) was maintained in RPMI 1640 HEPES (Gibco) supplemented with 10% FBS (Gibco) and 1X Antibiotics-antimycotics (Gibco). Mouse primary perivascular cells and mouse primary aorta endothelial cells were harvested as previously described[7] and expanded in DMEM high glucose supplemented with 20% FBS. HUVEC (human primary

endothelial cell) was obtained from Lonza, and cultured in EGM-2MV (Lonza). HUVEC were cultured in 1.5% gelatin-coated dishes. Human brain vessel pericyte (HBVP, purchased from ScienCell) was grown on poly-L-lysine coated dishes and maintained in Pericyte Medium (ScienCell).

Immunofluorescence analysis of mouse retina

Eyeballs including the optic nerve were taken from mice at the postnatal day 4 and 5 and 15 week. The eye and the retina were harvested, processed as previously described[8]. The retinae were stained with Lectin from Bandeiraea simplicifolia FITC conjugate (Sigma-Aldrich), anti-alpha-smooth muscle actin Cy3 conjugate (Sigma-Aldrich), anti-CD31 PE conjugate (BD Biosciences), anti-NG2 Alexa 488 conjugate (Millipore), anti-NG2 cy3 conjugate (Millipore), and anti-Collagen IV antibody (Millipore) where necessary and then examined under confocal microscopy (Zeiss).

In vitro angiogenesis assay

For Matrigel two-dimensional tube formation assay, confocal

dishes (Ibidi) were coated with 80 μl of GFR-Matrigel (Corning) and incubated for 30 minutes in 37° C incubator for polymerization. As for the ECs-pericytes co-culture experiment, $3x10^4$ MS1 and $1x10^4$ WT/Kai1 K/O mouse primary pericytes were then seeded on polymerized GFR-Matrigel with EBM 5% media. As for EC-conditioned medium set, $3x10^4$ MS1 was seeded on GFR-Matrigel coated μ-Dish (Ibidi) with conditioned media of primary pericytes from WT or *Kai1* K/O mouse. For three-dimensional spheroid sprouting assay, spheroids of pericytes, ECs and cancer cells combinations was generated using hanging drop. Spheroids seeded on polymerized GFR-Magrigel. For tube formation assay using overconfluent pericytes monolayer, high density of pericytes (10T1/2 cells) was incubated for 5 day in growth media and GFP expressing-ECs (MS1) was performed co-culture with pericytes monolayer for 3 day.

Tube formation Images were acquired using fluorescence microscopy and Zeiss LSM-710 META confocal microscope. Random fields were measured in terms of tube length and number of branching point by ImageJ (National Institutes of Health).

Adeno virus transduction

Adenovirus carrying mouse KAI1 was created with the pAdEasy vector system and titrated using the PFU (Plaque Forming Unit) assay. 10T1/2 cells transduced with adenovirus before used in experiments.

Gene expression analysis

Total RNA was extracted using TRIzol reagent (Invitrogen) or RNeasy mini kit (Qiagen) according to the manufacturer's instructions. Reverse transcription PCR was performed as previously described[3]. Briefly, cDNA was synthesized using a Primescript 1st strand cDNA synthesis kit (TAKARA) and oligo-dT primer. Semi-quantitative PCR was performed with Maxime PCR Pre-Mix (Intron) according to manufacturer's instructions and real-time PCR was performed with SyBR Green I Mastermix (Applied Biosystems) using an ABI PRISM TM 7500 Sequence Detection System (Applied Biosystems). Information of corresponding primers is provided in Table 1-3.

Western blot

Cells were lysed with lysis buffer (Cell Signaling) containing protease inhibitor (Roche). Total protein was immunoblotted with primary antibodies against KAI1, LIF (Santa Cruz Biotechnology), tSrc, pSrc (Tyr416) and pSrc (Tyr527), followed by incubation in HRP-conjugated secondary antibodies (Jackson Laboratories). Beta-actin (Santa Cruz Biotechnology) was used as an internal control.

Flow cytometry

Cells were collected in FACS buffer (dPBS (Gibco) containing 1% FBS and 0.1% BSA (Amresco)) as previously described[3]. Cells stained with antibodies specific for KAI1 (Miltenyi Biotec and Abcam), CD45 (BD Biosciences) and CD31 (BD Biosciences), PDGFRβ (Biolegend) and analyzed using a BD FACS Canto II (BD Biosciences) and were sorted using a BD FACS Aria (BD Biosciences) instrument. Appropriate isotype antibodies served as negative controls.

RNA sequencing

RNA sequencing was performed as previously described[3]. Briefly, RNA was extracted pericytes from WT and *Kai1* K/O mouse. GO (Gene Ontology) was performed using (http://geneontology.org/). Gene set enrichment analysis (GSEA) was used against custom-made lists from the GO (Gene Ontology).

Determining LIF concentrations in conditioned medium (ELISA)

LIF concentrations of conditioned media of adenovirus-transduced MS1 and 10T1/2 cells were determined using Mouse LIF Quantikine ELISA Kit (R&D Systems). Briefly, 1:2 diluted standard, control and samples were incubated for 2 hours at room temperature followed by a total of five washes. 100 μl of Mouse LIF Conjugate was added and incubated for 2 hours at room temperature, again followed by five washes. 100 μl of Substrate Solution was added and incubated for 30 minutes at room temperature in the dark. 100 μl of Stop Solution was added and optical density of each sample was determined using a microplate reader (Promega). Concentration was calculated by four

parameter logistic (4-PL) regression.

Immunofluorescence imaging

Cells were fixed in 2% paraformaldehyde (Wako) for 10 minute on ice. Mouse eyes (retina), upon removal, were immediately fixed in 4% paraformaldehyde for 1 hour at room temperature. After washed with PBS, samples were blocked with 1% BSA and 0.1% Triton X-100, followed by staining with primary antibodies against molecules of interest. When necessary, samples were incubated with secondary antibodies. The nucleus was stained with DAPI. For immunohistochemistry, samples were frozen in OCT embedding medium (Sakura) or embedded in paraffin, and then prepared as microscope slides, which were stained with appropriate primary and secondary antibodies.

Protein interaction assay

Real-time data showing the binding of KAI1 to VEGF-A and PDGF-BB was obtained with Blitz instrument (ForteBio). To illustrate, recombinant human rhKAI1 protein was bound to anti-Penta-His biosensors. Unbound rhKAI1 proteins were washed

away. 4 μL of rhVEGF-A, and PDGF-bb proteins was loaded, then binding to anti-Penta-His biosensors was measured in real time. Data was reference-subtracted using the negative control samples. Upward shifts indicate binding of two different proteins.

ABE assay

Mouse pericytes (101/2) and mECs (MS-1) were harvested by using palmitoylation lysis buffer (PLB) containing 1% NP-40 (Sigma), 10% Glycerol (Sigma), 50 mM N-ethylmaleimide (NEM, Sigma), 1 μM PMSF (Sigma), 200X PIC (Biovision), 50 mM Tris-HCl pH 7.4, and 150 mM NaCl. Lysates were briefly sonicated and incubated at 4° C for 24h, followed by centrifuging at 13,300 rpm 30 min. at 4° C. Then, the supernatant was subject to Chloroform-Methanol protein precipitation (4:1:3 = methanol : chloroform : water). Protein pellet was solubilized in 0.5% SDS buffer and briefly sonicated. Concentrated proteins were treated with 0.5 M hydroxylamine (Sigma, 159417) or Tris-HCl pH7.4 buffer (negative control) for 2 h at room temperature. Next, proteins were precipitated with following chloroform-methanol precipitation method, solubilized in 0.5% SDS, and then briefly

sonicated. Solubilized proteins were diluted with 1/10 dilution to make 0.05% SDS and immunoprecipitated with 40㎕ neutravidin (Invitrogen) for 2 h at 4° C. Immunoprecipitated beads were washed for three times with PLB and eluted with 2X DTT-containing SDS PAGE sample buffer (3 M).

Lipid raft isolation

Lipid raft isolation in mouse pericytes (10T1/2) and mECs (MS-1) was performed as previously described with minor[9]. For lipid-protein crosslinking, cells were treated with 1.25 mM DTSSP solution and incubated for 1h on ice at 4° C. Cells were washed with cold PBS and 5 mM EDTA and then added 0.75 mL cold PBS and 5 mM EDTA. Samples were frozen overnight at -80° C. Cells were lysed with 0.8 mL of 0.1% Triton X-100 membrane raft isolation buffer (1 M Tris-HCL, pH7.4, 1 M Nacl, 100 mM EDTA, Triton X-100, DW, protease inhibitor cocktail), a 23-gauge needle sing a 5-mL syringe 20x. 500 ㎕ supernatant was added 1 mL OptiPrep separation medium (60% iodixanol) (resulting it a 40% iodixanol solution of lysed cells). Using a Pasteur pipet, carefully overlay 40% iodixanol solution

with equal amounts of 30% iodixanol solution, and then 5% iodixanol solution. Gradient was visible to the naked eye. Samples were spinning in ultracentrifuge for 5 h at 132,000xg at 4° C. The membrane rafts were contained in the second fraction and visible. The subsequent process was the same as western blotting.

Statistical analysis

Continuous data are presented as the mean ± SEM and were compared using the two-tailed Student t test or the Mann-Whitney rank sum test, as appropriate. To compare multiple samples, statistical significance was assessed using a one-way ANOVA and adjustment for multiple comparisons was done using Tukey's t-test or Tamhane test, as appropriate. In all cases, multiple experiments were performed (number of experiments are shown in each figure) independently to verify the reproducibility. A two-sided probability value $p<0.05$ was considered statistically significant. Statistical tests were performed using the statistical package SPSS version 18 (SPSS Inc, Chicago, IL).

Table 1. Primer sequences for semi-quantitative RT-PCR [Mouse]

Primer	Sequence	Access Number
Kai1	Forward 5'-CACTACAACTGGACAGAGAACGAG	NM_007656.5
	Reverse 5'-TGTAGTCTTCAGAATGAATGTACCG	
Vegfa	Forward 5'-GGCTTTACTGCTGTACCTCCA	NM_001025250.3
	Reverse 5'-ACAGGACGGCTTGAAGATGTA	
Fgf2	Forward 5'-TGTGTCTATCAAGGGAGTGTGT	NM_008006.2
	Reverse 5'-GCTCTTAGCAGACATTGGAAGAA	
Pdgf-bb	Forward 5'-AGATTGAGATTGTGCGAAAGAAG	NM_011057.3
	Reverse 5'-GTCATGGGTGTGCTTAAACTTTC	
Ang2	Forward 5'-TGTTCCCAGATGCTCTCAGG	NM_007426.4
	Reverse 5'-GGATCATCATGGTTGTGGCC	
Esm1	Forward 5'-TGCTGACCACACTCCTGGTA	NM_023612.3
	Reverse 5'-TCCATGCCTGAGACTGTACG	
Vegfr2	Forward 5'-CTGGCAGCACGAAACATTCT	NM_010612.2
	Reverse 5'-AGACCACACATCGCTCTGAA	
Dll4	Forward 5'-TATTGGGCACCAACTCCTTC	NM_019454.3
	Reverse 5'-TCATTTTGCTCGTCTGTTCG	

Unc5b	Forward 5'-AGCAGCTGCCGTACTTCCTA Reverse 5'-TCCTGTGTGACGTGGTCATT	NM_029770.3
Apelin	Forward 5'-CTCTGGCTCTCCTTGACTGC Reverse 5'-TGTCTGCGAAATTTCCTCCT	NM_013912.4
Sox7	Forward 5'-TGTCCCAGAAGAGACCCTATGT Reverse 5'-ATGAGGACGAGAAGAAGGTCTG	NM_011446.1
Sox17	Forward 5'-GACCACCCCAACTACAAGTACC Reverse 5'-ATAGTCCGAGACTGGAGCGTAA	NM_011441.5
Sox18	Forward 5'-CCACTCGCAGGTCTCTACTATG Reverse 5'-CCTGAGATGCAAGCACTGTAAT	NM_009236.2
Lif	Forward 5'-TCATGAACCAGATCAAGAATCAA Reverse 5'-GATGGGAAGTCTGTCATGTTAGG	NM_008501.2
Gapdh	Forward 5'-CCCTTCATTGACCTCAACTACAT Reverse 5'-CATTGCTGACAATCTTGAGTGAG	NM_001289726.1

Table 2. Primer sequences for quantitative RT-PCR [Mouse]

Primer	Sequence	Access Number
Kai1	Forward 5'-CAGCTTCATTTCCGTCCTACA	NM_007656.5
	Reverse 5'-CACACCGATGAAGACGTAAGC	
Lif	Forward 5'-TCATGAACCAGATCAAGAATCAA	NM_008501.2
	Reverse 5'-CCCTTGAGCTGTGTAATAGGAAA	
Sulf1	Forward 5'-CCAAACGACACAATCCACTG	NM_001198565.1
	Reverse 5'-TGAAGGGGTGAAGGTGACTC	
Hoxa5	Forward 5'-AAAAACTCCCTGGGCAACTC	NM_010453.5
	Reverse 5'-TGGGCCACCTATATTGTCGT	
Optc	Forward 5'-TGAGGGGGTGTCTAGCTGTC	NM_054076.3
	Reverse 5'-TCTGAGGGAGGGGTAGGAGT	
Dhhc1	Forward 5'-GGCACAAGCTCACCACCTAT	NM_175160.3
	Reverse 5'-CTCCATCTCCTGAATGGACCG	
Dhhc2	Forward 5'-CTCTACTGGATCCCGGTGGT	NM_178395.3
	Reverse 5'-TGTTTTCCATGGACACTATGCAC	
Dhhc3	Forward 5'-AGGTGGTGTACAAGTGTCCC	NM_026917.5
	Reverse 5'-CACCGCTTACAAACACTGC	
Dhhc4	Forward 5'-CCGGTTTGGGCCGGTTC	NM_028379.5
	Reverse 5'-CAGATAGCAGCTCCGCTTGG	

Dhhc5	Forward 5'-GGAAAGAGGTTCAAACCCAGC Reverse 5'-GTCCTGGACACGTAAAGGCAA	NM_144887.4
Dhhc6	Forward 5'-CCAGACTGAGGCTGTGTTTCA Reverse 5'-GGGTCACTGAGGTGGGGTAT	NM_025883.3
Dhhc7	Forward 5'-GAGGGCCTCCTGTTCTTCAC Reverse 5'-CAGCCTCTCGATCTCTGTTTCA	NM_133967.3
Dhhc8	Forward 5'-CACTGGCTATGCAGAGGGAT Reverse 5'-GCCGGACACCTTCTTAACCA	NM_172151.4
Dhhc9	Forward 5'-TCAGGGAGAAGTCGCTACCA Reverse 5'-CAAGAGCCCTGAACAAGGGA	NM_172465.4
Dhhc10	Forward 5'-AAGAAGTTCCTACCACGCCC Reverse 5'-AACACCCCACCCATCACAATA	NM_027704.2
Dhhc11	Forward 5'- TGTGTCTGGATAAATAGCTGCG Reverse 5'- TCCGTAAACCGAAGTGAGCAA	NM_001007460.1
Dhhc12	Forward 5'-GACACCGAGCTACGCCAAT Reverse 5'-GGGGTCCATGAGTGACACAG	NM_001037762.1
Dhhc13	Forward 5'-AGCGATCGGAAAGCCGTTAC Reverse 5'-ATGGTCACGACGTAGGATGC	NM_001168516.1
Dhhc14	Forward 5'-CAGAGTGACATGTGCGACCA	NM_146073.3

	Reverse 5'-CAAGGTTGGGCATGGAGGAG	
Dhhc15	Forward 5'-TCTGTGTCTCCGACAGGAGC Reverse 5'-GCAGTCCAAACGGTGGCTTA	NM_175358.4
Dhhc16	Forward 5'-TGGGCCACTATAACCATCGC Reverse 5'-GGTACGTCTCAATGGCAGCA	NM_023740.2
Dhhc17	Forward 5'-TAACACCAAGATGGCGGACG Reverse 5'-TGGTTTGATTTCCTCCGGGT	NM_172554.2
Dhhc18	Forward 5'-TGCCTCCCAGCCTGATTGAC Reverse 5'-CAGGTGGCAAGCACATTCAG	NM_001017968.2
Dhhc19	Forward 5'-CCCTGGCCATGCCTTTCTTA Reverse 5'-GCCACCTACAAGGGAATCCG	NM_199309.2
Dhhc20	Forward 5'-GGATCATCACTGTCCATGGGT Reverse 5'-ACTGTTGGTTCATTCGTCCA	NM_029492.4
Dhhc21	Forward 5'-AGTGAATTTGCAAGTGGATTGTCT Reverse 5'-CAACCATGCGGGTCAACAAC	NM_026647.3
Dhhc22	Forward 5'-GCTCGCAGTGCAGGAATCAC Reverse 5'-TGTTTTCATGTACACAGATGCCG	NM_028031.3
Dhhc23	Forward 5'-TCCGGGACCTGCTTATACCA Reverse 5'-TGGCAGTCGGTACAGTAGGA	NM_027306.3

Dhhc24	Forward 5'-TTCTTCTCCGGAGCTGTCCT Reverse 5'-GATCAACAGCAGTTGGTGGC	NM_00108094 3.2
Gapdh	Forward 5'-TGTCCGTCGTGGATCTGAC Reverse 5'-CCTGCTTCACCACCTTCTTG	NM_00128972 6.1

Table 3. Primer sequences for semi-quantitative RT-PCR [Human]

Primer	Sequence	Access Number
LIF	Forward 5'-ACCGCATAGTCGTGTACCTT Reverse 5'-ACACGGCGATGATCTGCTTA	NM_002309.4
LIFR	Forward 5'-AGAGTGTCTGTGAGGGAAGC Reverse 5'-ATAACCTGTGCAGTCCCTCC	NM_001127671.1
GP130	Forward 5'-CAGCATCCAGTGTCACCTTT Reverse 5'-CCATCCCACTCACACCTCAT	NM_002184.3
GAPDH	Forward 5'-GGGTGTGAACCATGAGAAGTATGA Reverse 5'-CATATTTGGCAGGTTTTTCTAGACG	NM_002046.6

RESULTS

Kai1/Cd82 on pericytes shows anti-angiogenic effects

Kai1 knockout (*Kai1*$^{-/-}$) mice exhibited enhanced vascularization in postnatal 2 and 5 day, as demonstrated by the immunofluorescence (IF) imaging of the retinal vascular bed in these mice **(Fig. 1A)**. However, *Kai1*$^{-/-}$ mice from 15-week-old did not change significantly vascularization **(Fig. 1A)**. Moreover, *Kai1*$^{-/-}$ retinae displayed more filopodia **(Fig. 1B)** and fewer empty sleeves (*i.e.* less vessel regression) than did the retina of *wild-type* (WT) mice **(Fig. 1C)**.

To determine whether the ECs or pericytes are responsible for the enhanced angiogenesis in *Kai1*$^{-/-}$ mice, we analysed KAI1 expressing cells in vascular niche. To verify these KAI1 protein tracing, we generated transgenic mouse strains expressing the KAI1-GFP fusion protein using CRISPR system. Interestingly, KAI1 is predominantly expressed in the pericytes rather than EC of the KAI1-GFP mice retinae **(Fig. 1D)**. KAI1 is expressed in the pericytes of brain and heart **(Fig. 1E)**. Fluorescence-

activated cell sorting (FACS) revealed that 43% of PDGFRβ(+) pericytes is KAI1(+) cells in the bone marrow of the KAI1-GFP fusion transgenic mice, in contrast to merely 9% of ECs **(Fig. 1F)**. Additionally, we analysed the expression of this molecule in the primary aortic ECs and primary pericytes. Pericytes exhibited considerably higher KAI1 expression levels than did ECs **(Fig. 1G and 1H)**. Similar results were obtained from FACS analysis of human primary umbilical vein endothelial cells (HUVEC) versus human brain vessel pericytes (HBVPs) **(Fig. 1I)**. To evaluate the effects of perivascular KAI1 expression on angiogenesis, we co-cultured *Kai1*$^{-/-}$ pericytes with MS1 cells (mouse EC line) and found that the tube formation was significantly enhanced, compared to co-culture of WT pericytes and MS1 cells **(Fig. 1J)**. Conversely, *Kai1*-overexpressing (O/E) 10T1/2 cells (pericytes line) were shown to suppress ECs sprouting **(Fig. 1K)**. To confirm the cell of origin for KAI1 to inhibit angiogenesis, we prepared mock- or *Kai1*-O/E MS1 or 10T1/2 cells for tube formation assay under various combinations of co-culture. We found that the over-expression of *Kai1* in the pericytes led to a strong suppression of tube

formation, while that in the MS1 cells had a relatively weak effect (Fig. 1L).

KAI1 localizes at the lipid rafts of pericytes, which depends on palmitoylation

To understand the different effects of KAI1 in ECs and pericytes, we checked KAI1 localization. Interestingly, surface expression of KAI1 was shown to be much higher on pericytes than that on the ECs (Fig. 2A). Next, we performed subcellular fractionation such as lipid-raft membrane, non-lipid raft membrane, and cytosolic proteins in ECs and pericytes. Endogenous KAI1 was detectable in membranous and cytosolic fraction in pericytes, while it was very low in ECs (Fig. 2B). When *Kai1-GFP* was introduced, both pericytes and ECs expressed KAI1 in cytosolic fraction. Interestingly, however, KAI1 expression at membranous or lipid-raft fraction was different, strong in pericytes and very weak in ECs (Fig. 2C). Expression of KAI1 in the lipid raft on pericytes rather than on ECs was confirmed by analysing the expression of a lipid raft marker, cholera toxin B,

and its co-localization with KAI1 on pericytes (Fig. 2D). Two different types of the lipid raft were reported, flotillin-enriched planar lipid rafts or caveolin-enriched caveolae[10]. We found that pericytes have flotillin-enriched planar lipid rafts while ECs have caveolae type ones (Fig. 2B and 2C).

Next we tried to decipher the mechanism how KAI1 is localized at lipid raft membranous fraction of pericytes, but not ECs. Palmitoylation is an important mechanism to regulate functions of the tetraspanin family members including CD9, CD81, KAI1/CD82, and CD151. KAI1 is palmitoylated at cytoplasmic cysteine residues, and then localized at cell membrane[11]. It is known that the functions of KAI1 depend on its palmitoylation status[11,12]. Therefore, we hypothesized that the different distribution or effect of KAI1 between ECs and pericytes is due to the different status of KAI1 palmitoylation between these cells. To detect the palmitoylated KAI1 molecules in the ECs and pericytes, we performed acyl-biotin exchange (ABE) assay. Palmitoylation level of KAI1 was shown to be significantly higher in the pericytes than in ECs (Fig. 2E). Protein palmitoylation is

catalysed by DHHC palmitoyl transferases, which contain cysteine-rich domains (CRDs)[10]. Members of the zDHHC family, except for zDHHC12, were shown to be expressed in pericytes more than in ECs **(Fig. 2F)**. We demonstrated that KAI1 directly interacts with zDHHC3 and zDHHC4 among 23 zDHHC enzymes screened **(Fig. 2G)**. To evaluate KAI1 palmitoylation by these two enzymes, we performed ABE assay following the knockdown of these genes. Interestingly, KAI1 palmitoylation was reduced by zDHHC4 knockdown, but not by zDHHC3 knockdown **(Fig. 2H)**. Inhibition of palmitoylation using 2-bromopalmitate (2-bp) significantly inhibited the KAI1 localization in lipid raft or membrane of pericytes **(Fig. 2I and 2J)**.

KAI1 induces LIF through Src/p53 axis, which turns angiogenic genes down

To investigate the mechanisms how KAI1 functions as a negative regulator of angiogenesis, we analysed the transcriptome of WT and *Kai1*$^{-/-}$ pericytes and performed gene set enrichment analysis (GSEA). We found that *Kai1*$^{-/-}$ pericytes showed a

significantly lower expression of "negative angiogenic regulators" (GO: 0016525) and "blood vessel remodelling genes" (GO: 0001974) than the control cells did **(Fig. 3A)**.

Among top 17 of "negative angiogenic regulators" (GO: 0016525), *Sulf1* and *Lif* levels considerably decreased in *Kai1*$^{-/-}$ pericytes less than 20% of control cells **(Fig. 3B)**. Interestingly, *Leukemia inhibitory factor* (*Lif)* that is included both in the negative regulators of angiogenesis and the blood vessel remodelling genes **(Fig. 3A and 3C)** emerged as one of the leading edge subset that contributes to the enrichment score (ES)[13]. Furthermore, a previous study reported that *Lif*$^{-/-}$ mice have increased endothelial filopodia, branching points, and capillary density in retina[14], which is very similar to our findings of *Kai1*$^{-/-}$ mice. Thus we examined *Lif* expression in pericytes and ECs after *Kai1* O/E, and found that *Kai1* significantly increased mRNA levels of *Lif* in pericytes, but not ECs **(Fig. 3D)**. Protein LIF concentration in the conditioned medium obtained form *Kai1*−O/E pericytes was shown to be higher than that in the medium obtained from control cells **(Fig. 3D)**. Baseline

expression level of Lif was also high in pericytes than in ECs in mouse as well as human cells, however, the expression level of its receptor Lifr was comparable between pericytes and ECs in both species **(Fig. 3E)**. To examine the functional relevance of LIF during angiogenesis, we performed tube formation after neutralization of LIF in the supernatant of *Kai1*−O/E pericytes (10T1/2). Of interest, supernatant of Kai1−O/E pericytes (10T1/2) inhibit the tube formation of endothelial cells (MS1), which were reversed by neutralization of LIF **(Fig. 3F)**.

To further investigate the relevance of LIF in angiogenesis, we examined the effect of the recombinant mouse LIF (rmLIF) on the expression of angiogenic genes in the mouse ECs and pericytes. LIF significantly suppressed expression of angiogenic genes, such as, *Ang2*, *Esm1*, *Dll4,* and *Vegfr2 in ECs* **(Fig. 3G)**. In the previous study, these genes are upregulated by Sox F family[15] that plays an important role in the vascular system development[16]. We found that LIF significantly suppressed *Sox17*, but not *Sox7* or *Sox18*, in ECs **(Fig. 3G)**. Meanwhile in pericytes, LIF suppressed *Vegfa* expression, but not *Fgf2* or

Pdfgb, in pericytes **(Fig. 3H)**.

We investigated the signalling pathways of KAI1–LIF axis in pericytes. Among inhibitors of several signaling pathways, Src inhibitor near–completely blocked the induction of *Lif* mRNA by *Kai1* O/E in pericytes **(Fig. 3I)**. In *Kai1*$^{-/-}$ pericytes, active form of Src is lower (phosphorylation at tyrosine 416 of Src) whereas inactive form of Src is higher (phosphorylation at tyrosine 527 of Src) than in WT cells. In *Kai1 O/E* pericytes, the opposite results were obtained **(Fig. 3J)**. Next, I evaluate the downstream of KAI1/Src pathway by examining transcription factor binding sites of *Lif* promoter region. A consensus p53–binding element in mouse *Lif* gene was previously reported at position +4547 (p53 binding site 2)[17]. Then I found an additional p53–binding element in this gene at position –269 (p53 binding site 1) from the transcription start site using prediction program. Additionally, consensus Pbx1 binding element in *Lif* gene confirmed using prediction program. Interestingly, we found that KAI1 induced binding of p52 at –269 position of *Lif* gene promoter, which was reversed by Src inhibitor **(Fig. 3K)**. However, Pbx1 binding on

Lif promoter by *Kai1* O/E induced Src pathway independent (Fig. 3K).

KAI1 binds to VEGF-A and PDGF-BB, but not to bFGF, leading to inhibition of VEGF/PDGF signalling

Previously, anti-KAI1 antibody was shown to inhibit VEGF signalling by regulating KAI1 distribution in the lipid rafts[18]. We hypothesised that KAI1 binds VEGF or VEGR directly, resulting in inhibition of VEGF signalling. Excitingly, recombinant human KAI1 (rhKAI1) bound to recombinant human VEGF (rhVEGF) and rhPDGF-BB, but not rhFGF2 (Fig. 4A-4C). Binding of KAI1 with VEGF or PDGF results in sequestration of angiogenic cytokines leading to inhibition of VEGFR2 and PDGFR phosphorylation in HUVECs and HBVPs even in the presence of VEGFA or PDGF-BB (Fig. 4D). Additionally, rhKAI1 dose-dependently inhibited endothelial cell tube formation (Fig. 4E). Taken together, KAI1 shows anti-angiogenic effects by two mechanism. First, KAI1 induces LIF through Src/p53 axis, which turns angiogenic genes down. Second, KAI1 binds to VEGF-A and PDGF-BB, leading to inhibition of VEGF/PDGF signalling.

(Fig. 4F)

Kai1 has therapeutic potential to inhibit tumour angiogenesis and growth

To investigate the therapeutic potential of rhKAI1 against cancer growth, we first examined the anti-angiogenic role of rhKAI1 using three-dimensional hybrid spheres consisting of cancer and blood vessel cells (melanoma cells, ECs, and pericytes). Spheres treated with rhKAI1 showed a reduced activity of sprouting compared with that treated with vehicle (Fig. 5A). To investigate the therapeutic potential of KAI1 to inhibit cancer growth in vivo mice model, we subcutaneously transplanted B16 (mouse melanoma cancer cells) and PC3 (human prostate cancer cells) without versus with KAI1 supplementation (combination of rhKAI1 and supernatant from *Kai1*-O/E pericytes). *In vivo*, tumour growth was remarkably retarded by supplementation of KAI1 (Fig. 5B and 5C). In the histologic examination, vessel formation in tumours was significantly decreased by supplementation of KAI1 (Fig. 5D). Therefore, rhKAI1 has a potential to prevent cancer angiogenesis and tumour growth (Fig.

5E).

Fig. 1

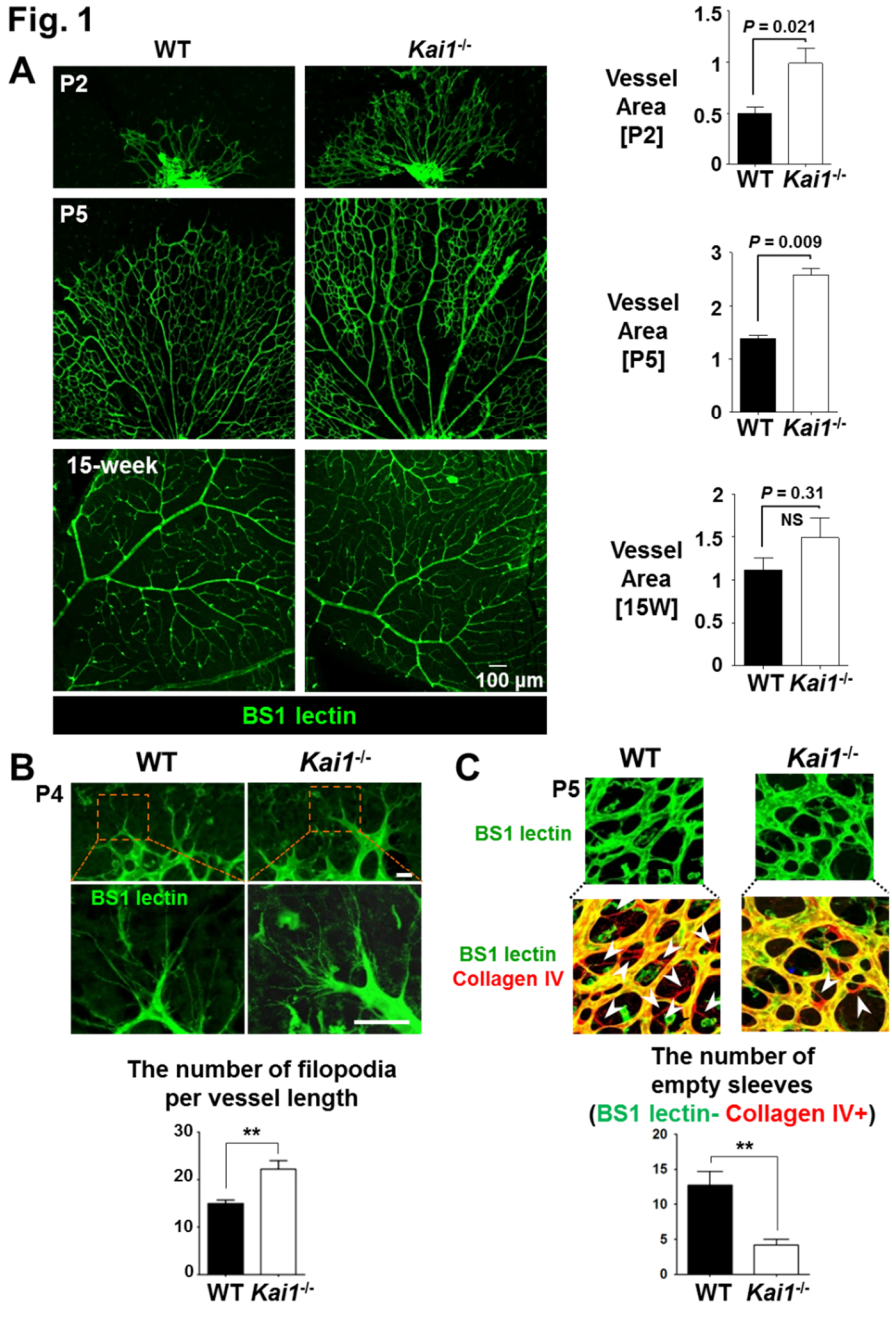
A
WT
Kai1-/-
P2
P5
15-week
100 μm
BS1 lectin
Vessel Area [P2]
P = 0.021
Vessel Area [P5]
P = 0.009
Vessel Area [15W]
P = 0.31
NS
WT Kai1-/-
B
P4
WT
Kai1-/-
BS1 lectin
The number of filopodia per vessel length
**
C
P5
BS1 lectin
BS1 lectin
Collagen IV
The number of empty sleeves
(BS1 lectin- Collagen IV+)
**

Fig. 1 (Continued)

D

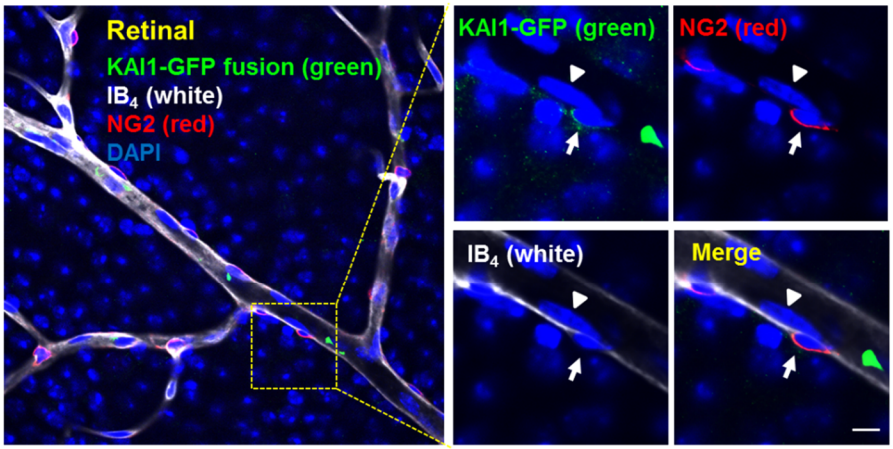

E

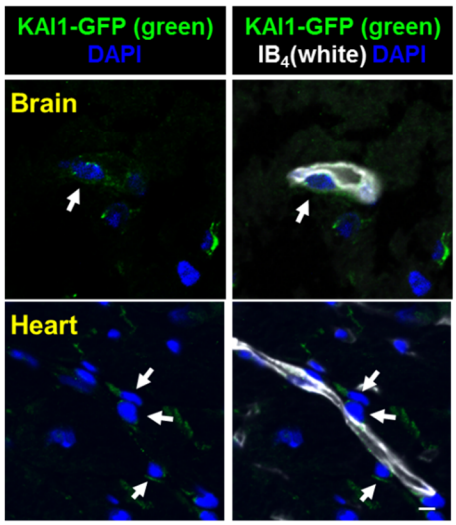

F

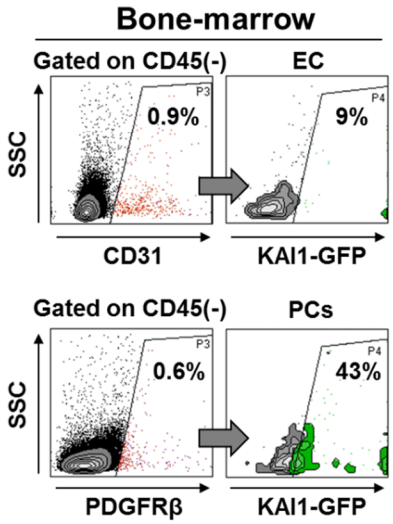

Fig. 1 (Continued)

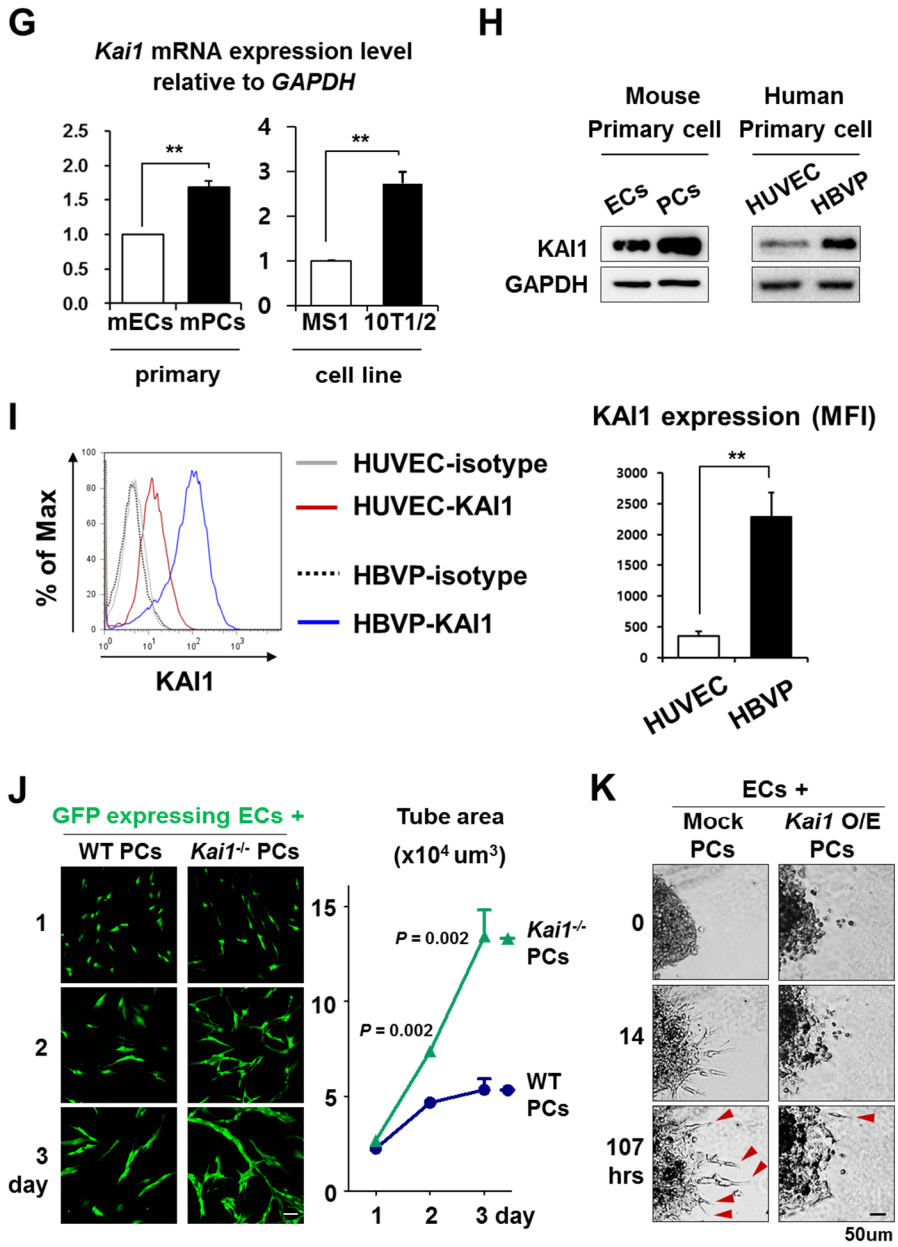

Fig. 1 (Continued)

L

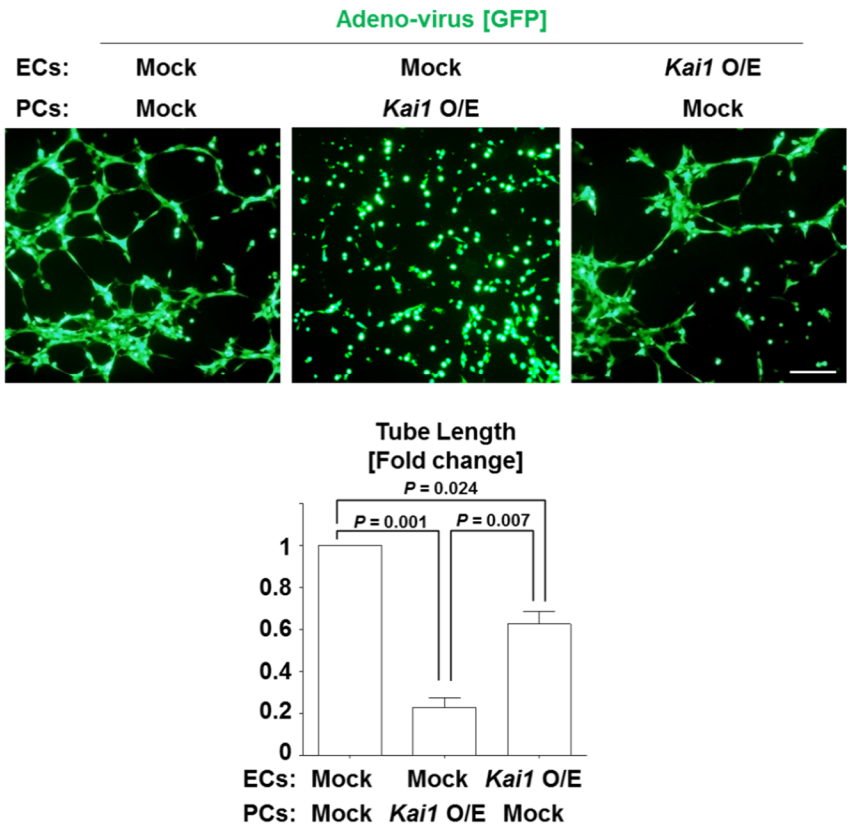

Figure 1. KAI1 on pericytes have anti-angiogenic effects.

(A) Left, retinal vasculature of the *wild-type* (WT) and *Kai1* knockout ($Kai1^{-/-}$) mice (postnatal day 2 and 5, and at 15 weeks of age). Endothelial cells were stained with BS-I lectin. Scale bar, 50 μm. **Right,** quantification of the obtained results (**p<0.05, scale bar, 100 μm). **(B) Top,** filopodia of the WT and $Kai1^{-/-}$ postnatal retinal vessels (postnatal day 4). Scale bar, 20

μm. **Bottom,** quantification of the obtained results (**p<0.05). **(C) Top,** vessel regression (empty sleeves, BS-1 lectin-negative, collagen IV-positive) in the WT and *Kai1*$^{-/-}$ mice. Arrowheads, empty sleeves. Scale bar, 50 μm. **Bottom,** quantification of the obtained results. **(D)** Tracking of KAI1 expressing cells in retinae of the KAI1-GFP fusion transgenic mice. Confocal images of Isolectin B4-(IB4, white) NG2- (red). **Right,** High-magnification images of the boxed area in the left figure. KAI1 was expressed in NG2(+)pericytes (Arrow), but not ECs (Arrowhead). Scale bar, 5 μm. **(E)** Confocal imaging of KAI1-GFP expression in brain and heart of the KAI1-GFP fusion transgenic mice. Scale bar, 5 μm. **(F)** FACS plot showing ECs ($CD45^{-}CD31^{+}$) and pericytes ($CD45^{-}PDGFR\beta^{+}$) in the bonemarrow of KAI1-GFP fusion transgenic mice. **(G)** *Kai1* expression in mouse primary ECs and mouse primary pericytes (**p<0.05). **(H)** KAI1 protein expression in the mouse primary ECs, mouse primary pericytes, HUVECs and HBVPs. **(I) Left,** KAI1 surface expression of HUVECs and HBVP, analyzed using FACS. **Right,** quantification of the obtained results (**p<0.05). **(J) Left,** i*n vitro* tube formation assay using GFP-MS1 cells co-

cultured with *Kai1*$^{-/-}$ or WT pericytes. Scale bar, 100 μm. . **Right,** quantification of the obtained results **(K)** *In vitro* Matrigel tube formation assay, performed using cellular spheroids, consisting of MS1 and 10T1/2 cells, transduced with the indicated adenovirus at 0, 14, and 107 h, and observed using time-lapse microscopy. Scale bar, 50 μm. **(L) Top,** *in vitro* tube formation assay in MS1 and 10T1/2 co-cultured cells, transduced with the indicated adenovirus. Scale bar, 200 μm. **Bottom,** quantification of the obtained results.

Fig. 2

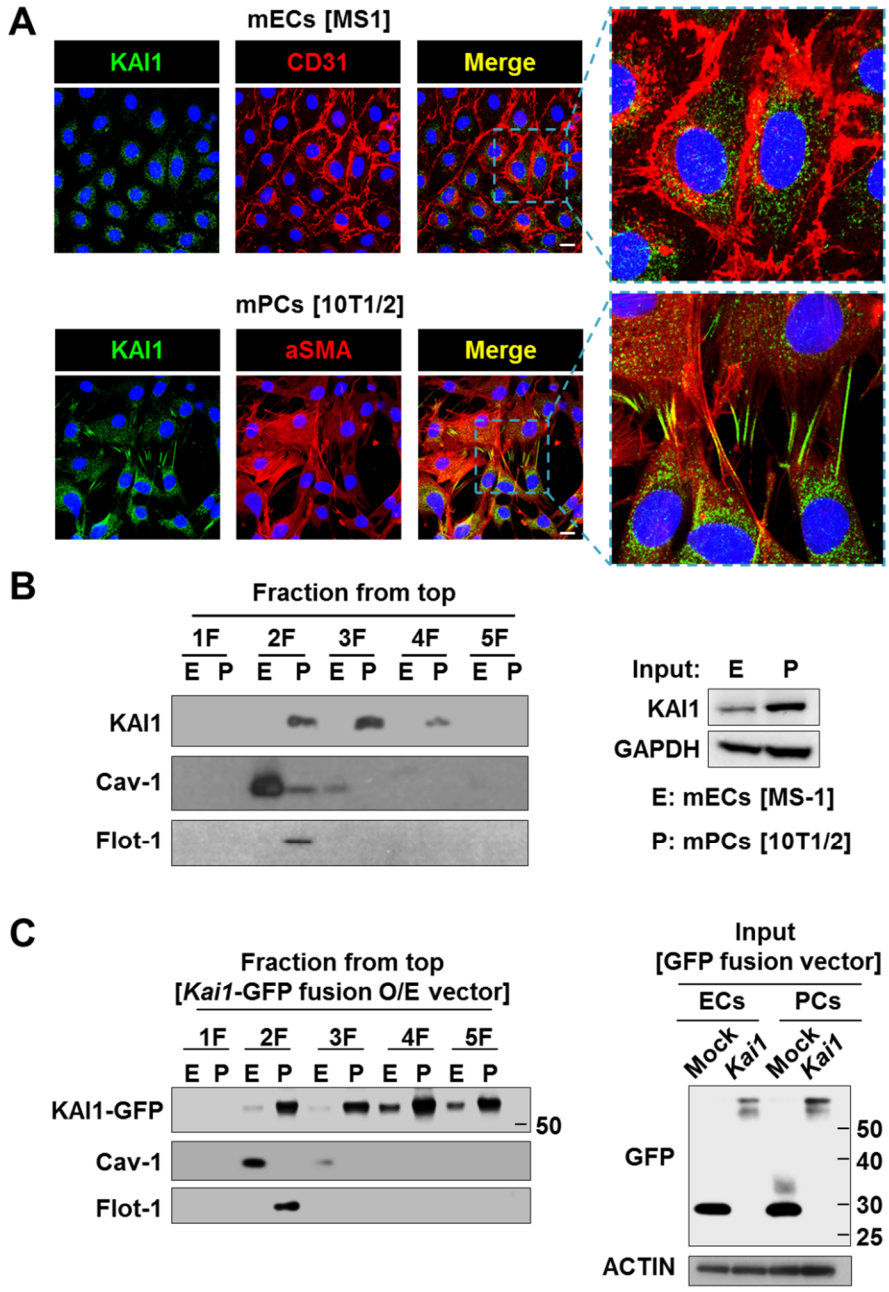
A
mECs [MS1]
KAI1
CD31
Merge
mPCs [10T1/2]
KAI1
aSMA
Merge
B
Fraction from top
1F 2F 3F 4F 5F
E P E P E P E P E P
KAI1
Cav-1
Flot-1
Input: E P
KAI1
GAPDH
E: mECs [MS-1]
P: mPCs [10T1/2]
C
Fraction from top
[Kai1-GFP fusion O/E vector]
1F 2F 3F 4F 5F
E P E P E P E P E P
KAI1-GFP
Cav-1
Flot-1
50
Input
[GFP fusion vector]
ECs PCs
Mock Kai1 Mock Kai1
GFP
50
40
30
25
ACTIN

Fig. 2 (Continued)

D

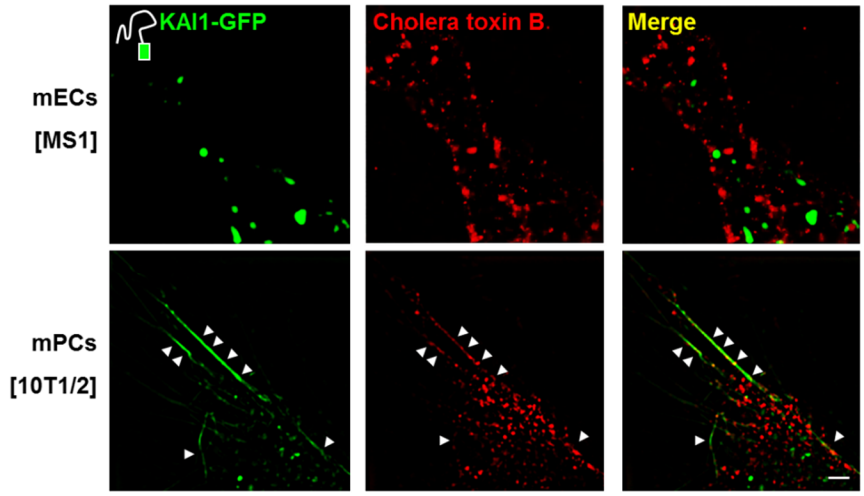

E

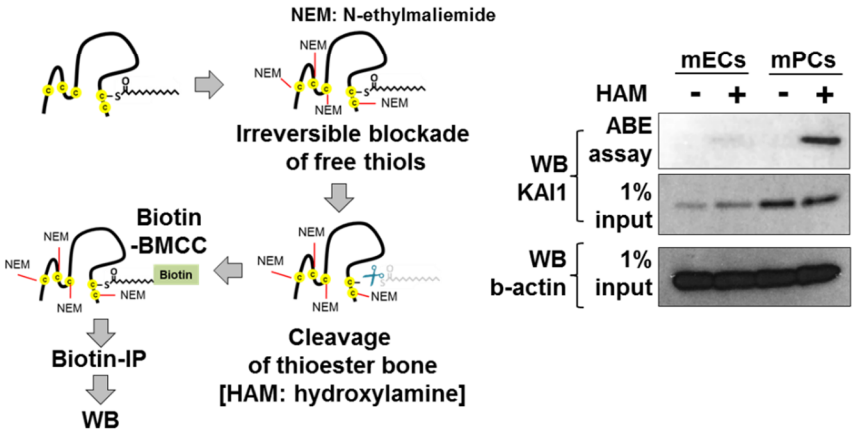

Fig. 2 (Continued)

F

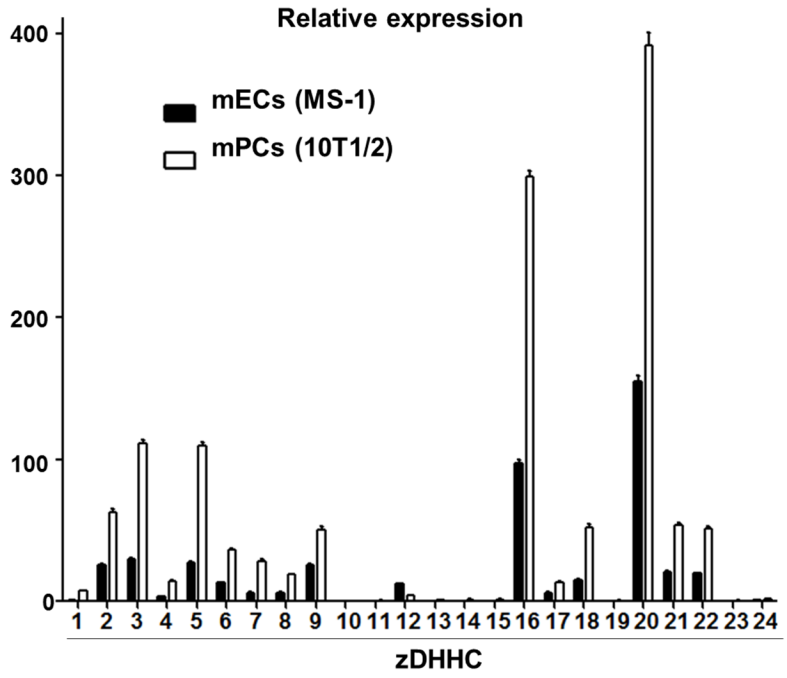

G

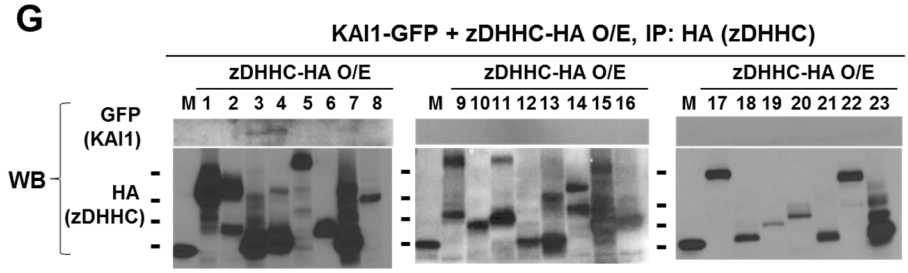

Fig. 2 (Continued)

H

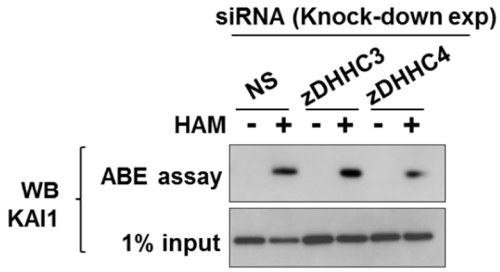

I

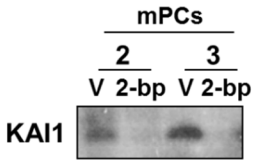

J

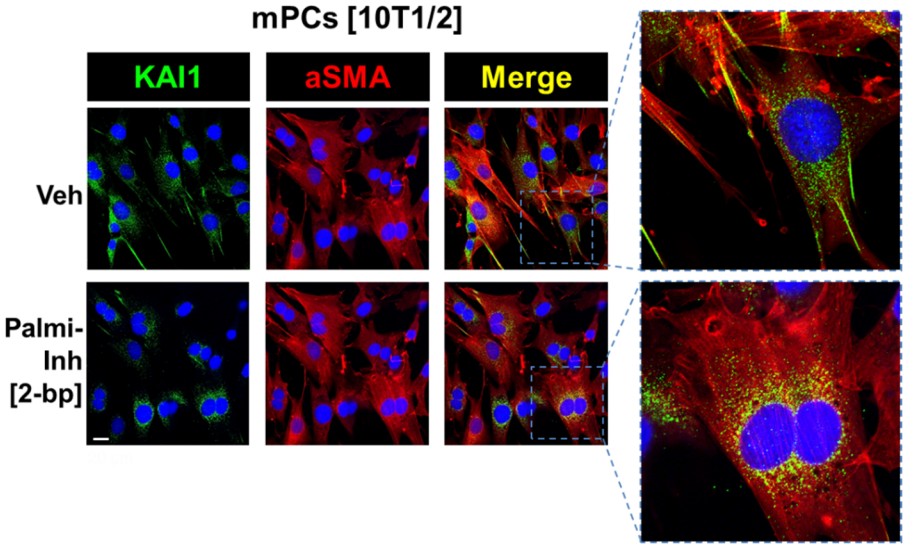

Figure 2. KAI1 localize to the lipid rafts of pericytes

(A) KAI1 localization confirmed in MS1 (endothelial cell line) and 10T1/2 (perivascular cell line) cells using immunofluorescence. Scale bar, 20 μm. (B) Lipid rafts isolated from MS1 and 10T1/2 cells using OptiPrep medium (frozen and crosslinks method) and KAI1 localisation confirmed. Flotillin-1 and caveolin-1 was detected lipid-raft membrane fraction. Fraction 2; Lipid raft proteins. Fraction 3; Non-raft membrane proteins. Fraction 4 and 5; Cytosolic proteins. (C) Lipid rafts isolated from MS1 and 10T1/2 cells transfected with *Kai1*-GFP fusion vector using OptiPrep medium (frozen and crosslinks method). Flotillin-1 (planar type) and caveolin-1 (caveolae type) was detected lipid-raft membrane fraction. Fraction 2; Lipid raft proteins. Fraction 3; Non-raft membrane proteins. Fraction 4 and 5; Cytosolic proteins. (D) Lipid raft marker (cholera toxin B, red) expression on MS1 and 10T1/2 cells transfected with *Kai1*-GFP fusion vector, observed using structured illumination microscopy. Arrowheads, co-localization of Kai1 protein and cholera toxin B. Scale bar, 2 μm. (E) KAI1 palmitoylation in MS1 and 10T1/2 cells confirmed using ABE assay. (F) *Zdhhc* family member

expression in MS1 and 10T1/2 cells. **(G)** *Zdhhc3* and *Zdhhc4* binding to KAI1, confirmed by co-immunoprecipitation. **(H)** *Zdhhc3* and *Zdhhc4* knockdown in mouse pericytes, and their effects on KAI1 palmitoylation levels. **(I)** Changes in KAI1 localization in the lipid rafts (Fraction 2) and non-lipid raft membrane (Fraction 3) following the inhibition of palmitoylation. **(J)** Changes in KAI1 localization after palmitoylation inhibition. Scale bar, 20 μm.

Fig. 3

A

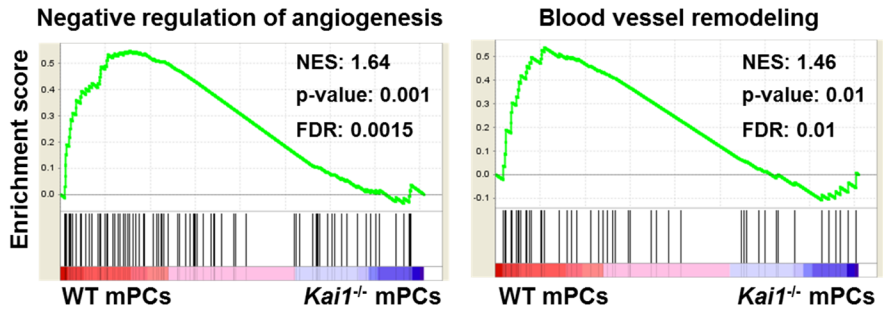
Negative regulation of angiogenesis
Blood vessel remodeling
Enrichment score
NES: 1.64
p-value: 0.001
FDR: 0.0015
NES: 1.46
p-value: 0.01
FDR: 0.01
WT mPCs
Kai1-/- mPCs
WT mPCs
Kai1-/- mPCs

B

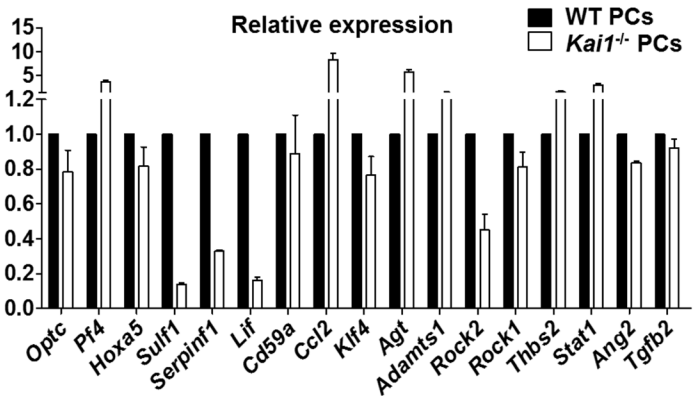
Relative expression
WT PCs
Kai1-/- PCs
Optc
Pf4
Hoxa5
Sulf1
Serpinf1
Lif
Cd59a
Ccl2
Klf4
Agt
Adamts1
Rock2
Rock1
Thbs2
Stat1
Ang2
Tgfb2

C

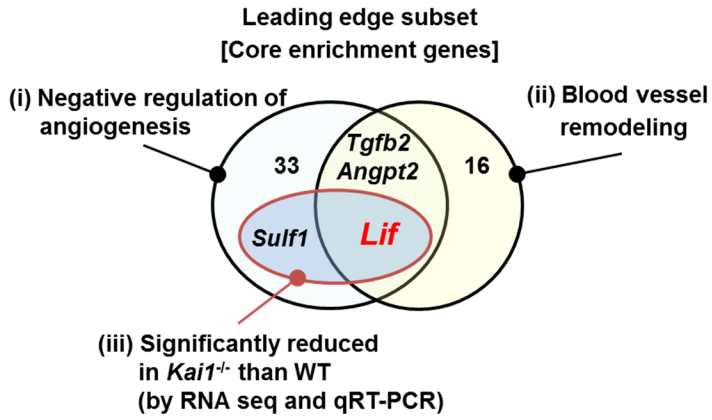
Leading edge subset
[Core enrichment genes]
(i) Negative regulation of angiogenesis
(ii) Blood vessel remodeling
33
Tgfb2
Angpt2
16
Sulf1
Lif
(iii) Significantly reduced in Kai1-/- than WT (by RNA seq and qRT-PCR)

Fig. 3 (Continued)

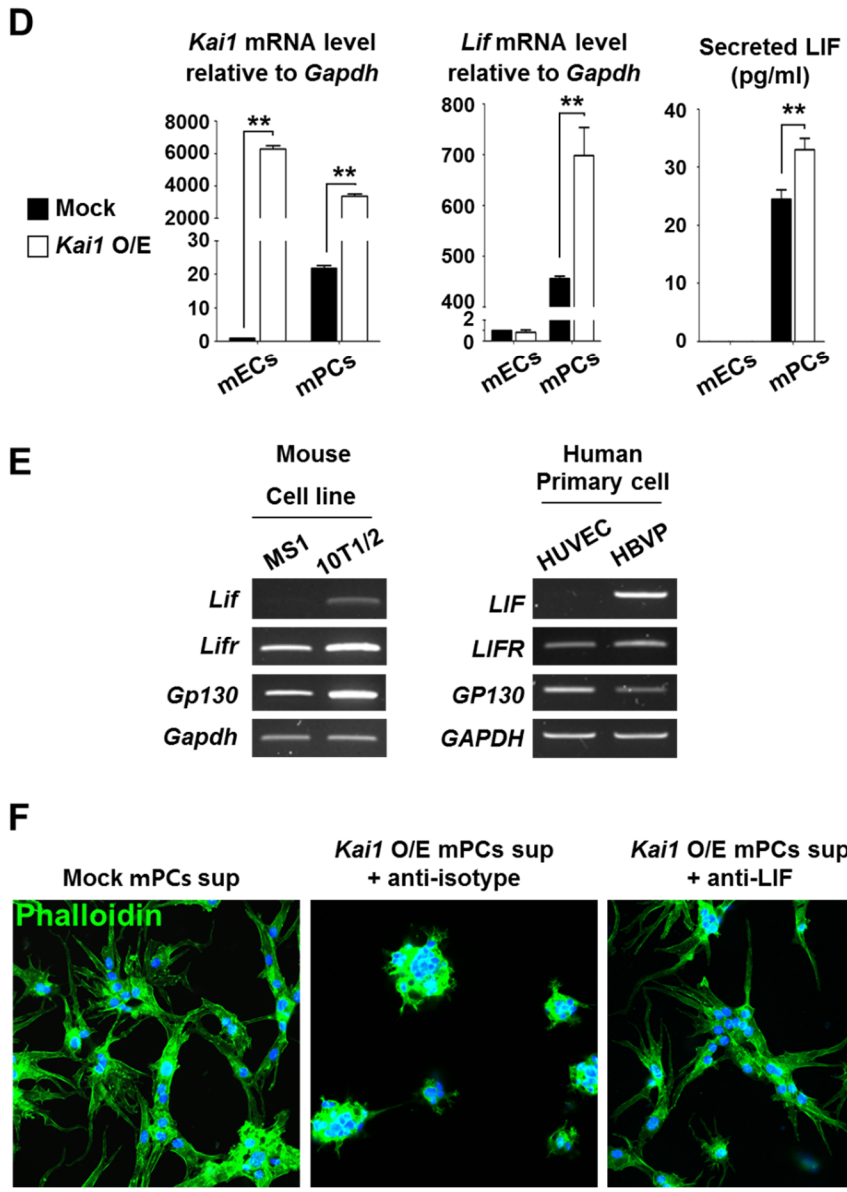

Fig. 3 (Continued)

G

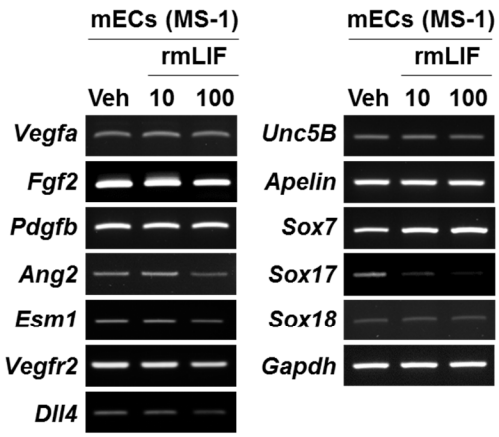

H

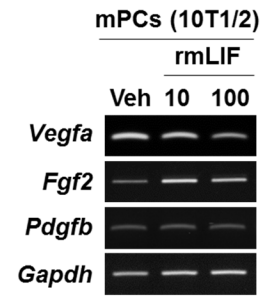

I

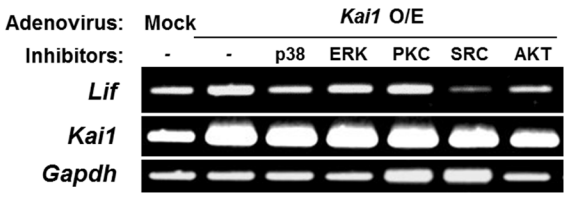

J

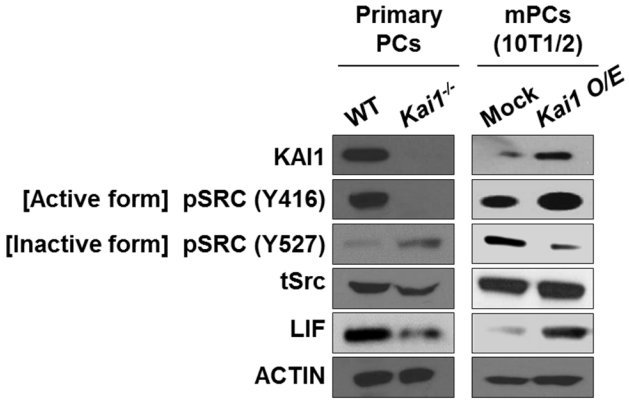

Fig. 3 (Continued)

K

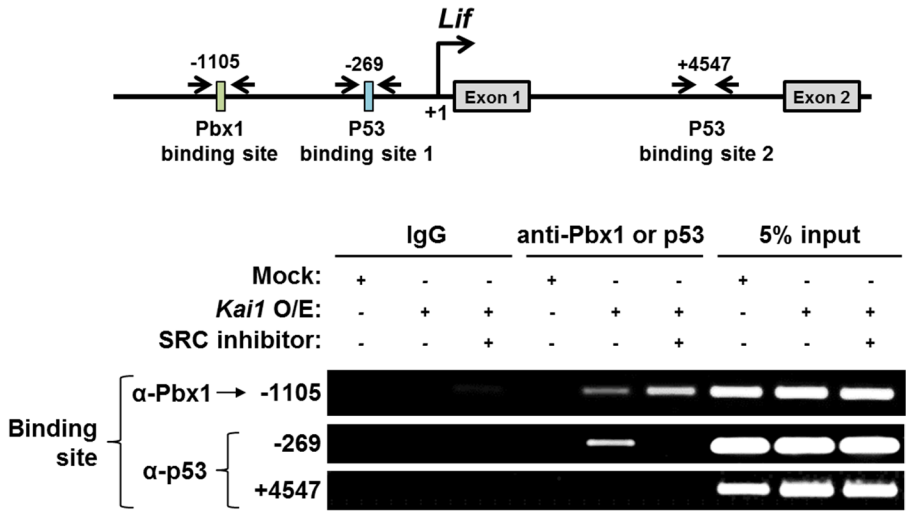

Figure 3. Anti-angiogenic LIF is the downstream effector molecule of KAI1 in pericytes. (A) GSEA of the negative angiogenic regulators (GO: 0016525) and blood vessel remodelling (GO: 0001974), based on the RNA-sequencing of WT and *Kai1*$^{-/-}$ pericytes. (B) mRNA levels for top 17 of "negative angiogenic regulators" in WT and *Kai1*$^{-/-}$ pericytes. (C) Venn diagram showing the leading edge subset (core enrichment genes) of GSEA data for negative angiogenic regulators (GO: 0016525) and blood vessel remodelling (GO: 0001974), based on the RNA-sequencing of WT and *Kai1*$^{-/-}$ pericytes. (D) *Kai1* and *Lif* expression in the *Kai1*-O/E MS1 and

10T1/2 cells (**p<0.05). **Right**, LIF level determination in the conditioned media of *Kai1*-O/E MS1 and 10T1/2 cells (**p<0.05). (**E**) *LIF*, *LIFR,* and *GP130* expression in mouse and human ECs and pericytes. (**F**) Tube formation assay using MS1 cells cultured in the conditioned media obtained from the control and *Kai1*-O/E 10T1/2. These media were treated with control IgG or anti-LIF antibody. Scale bar, 50 μm. (**G**) Changes in the levels of angiogenic molecules (*Vegfa, Fgf2, Pdgfb, Ang2, Esm1, Vegfr2, Dll4, Unc5B, Apelin, Sox7, Sox17,* and *Sox18*) in MS1 cells following the treatment with Lif (10 and 100 ng/mL). (**H**) Changes in *Vegfa, Fgf2,* and *Pdgfb* levels in 10T1/2 cells in response to the Lif treatment (10 and 100 ng/mL). (**I**) *Lif* and *Kai1* expression in 10T1/2 cells pre-treated with p38, Erk, Pkc, Src, and Akt inhibitors and then transduced with *Kai1*-O/E using adenovirus. (**J**) Src phosphorylation levels and positions and LIF immunoblotting results in **left**, WT and *Kai1*$^{-/-}$ pericytes and, **right**, control and *Kai1*-O/E pericytes (10T1/2). (**K**) **Top**, scheme, showing the regions targeted with the chromatin immunoprecipitation (ChIP) assay. **Bottom**, binding of p53 and Pbx1 on Lif promoter region using ChIP assay.

Fig. 4

A

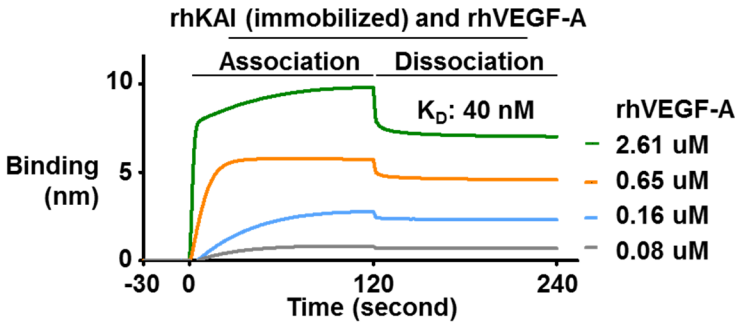
rhKAI (immobilized) and rhVEGF-A
Association
Dissociation
K_D: 40 nM
rhVEGF-A
2.61 uM
0.65 uM
0.16 uM
0.08 uM
Binding (nm)
10
5
0
-30
0
120
240
Time (second)

B

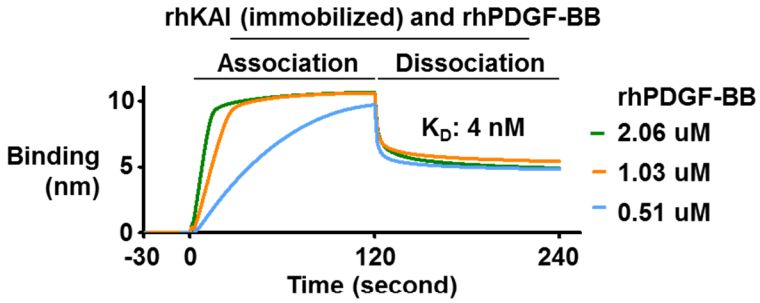
rhKAI (immobilized) and rhPDGF-BB
Association
Dissociation
K_D: 4 nM
rhPDGF-BB
2.06 uM
1.03 uM
0.51 uM
Binding (nm)
10
5
0
-30
0
120
240
Time (second)

C

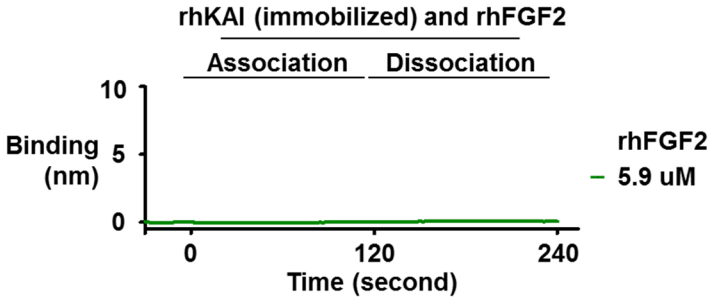
rhKAI (immobilized) and rhFGF2
Association
Dissociation
rhFGF2
5.9 uM
Binding (nm)
10
5
0
0
120
240
Time (second)

Fig. 4 (Continued)

D

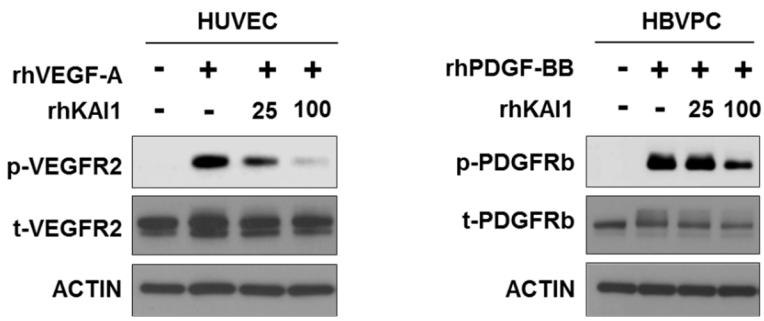

E

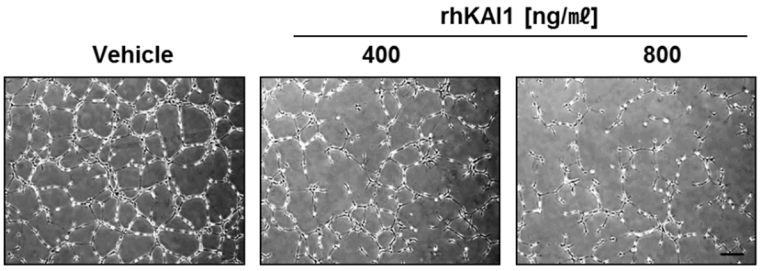

F

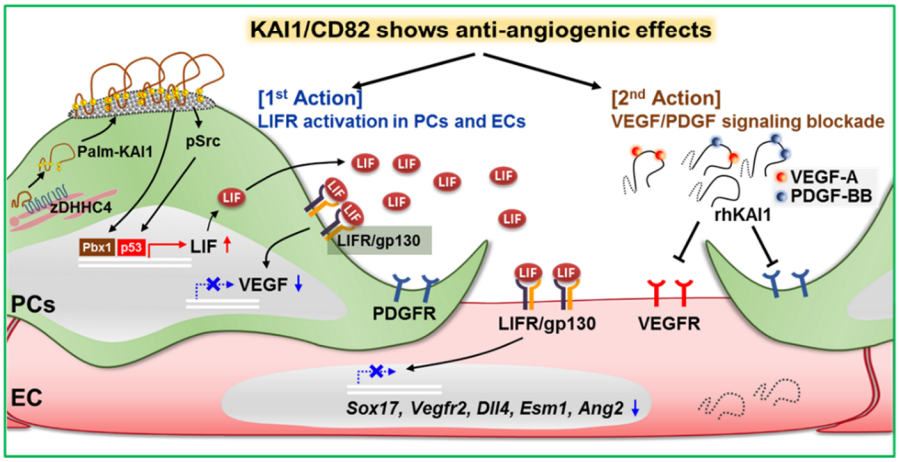

Figure 4. rhKAI1 binds VEGF-A and PDGF-BB directly, resulting in inhibition of VEGFR2 and PDGFRb signalling. (A-C) Protein-protein interactions between rhKAI1, rhVEGFA (A), PDGF-BB (B) and FGF2 (C) observed using surface plasmon resonance (BLItz system). A shift in nm indicates the binding of two proteins. (D) **Left**, VEGFR2 phosphorylation levels in HUVECs, in response to VEGFA and rhKAI1 treatment. **Right**, PDGFR-β phosphorylation level in human brain vascular pericytes (HBVP), in response to PDGF-BB and rhKAI1 treatment. (E) Matrigel tube formation assay using HUVECs treated with pro-angiogenic cytokines, VEGF-A and PDGF-BB, following the treatment with bovine serum albumin or rhKAI1 (400 and 800 ng/mL). Scale bar, 500 μm. (F) Schematic figure showing the role of KAI1 in angiogenesis.

Fig. 5

A

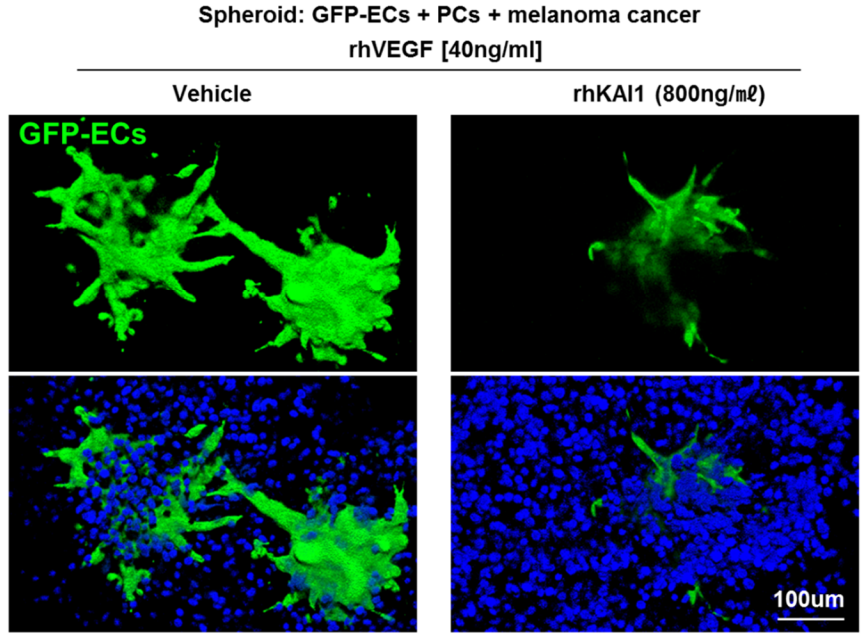
Spheroid: GFP-ECs + PCs + melanoma cancer
rhVEGF [40ng/ml]
Vehicle
rhKAI1 (800ng/㎖)
GFP-ECs
100um

B

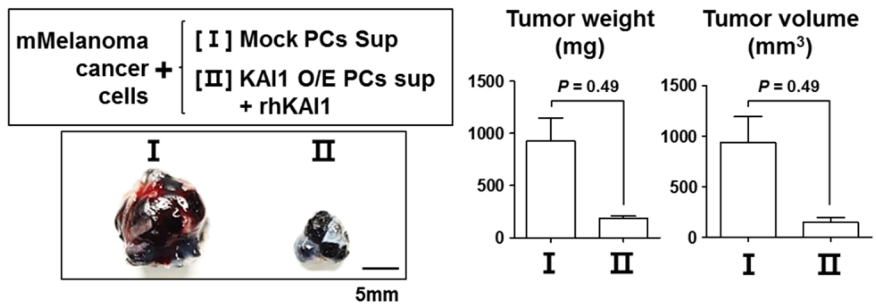
mMelanoma cancer cells +
[Ⅰ] Mock PCs Sup
[Ⅱ] KAI1 O/E PCs sup + rhKAI1
Ⅰ
Ⅱ
5mm
Tumor weight (mg)
Tumor volume (mm3)
P = 0.49
P = 0.49
1500
1000
500
0
Ⅰ
Ⅱ

Fig. 5 (Continued)

C

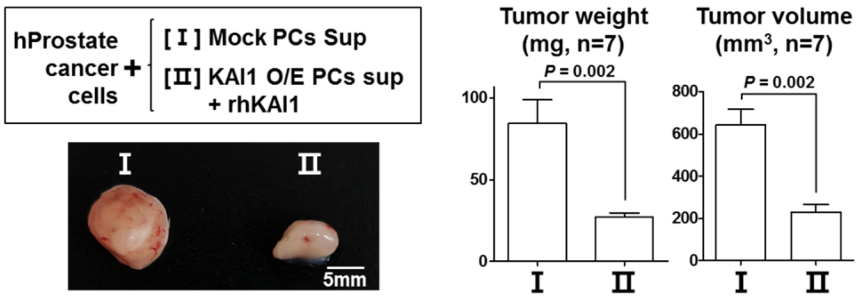

D

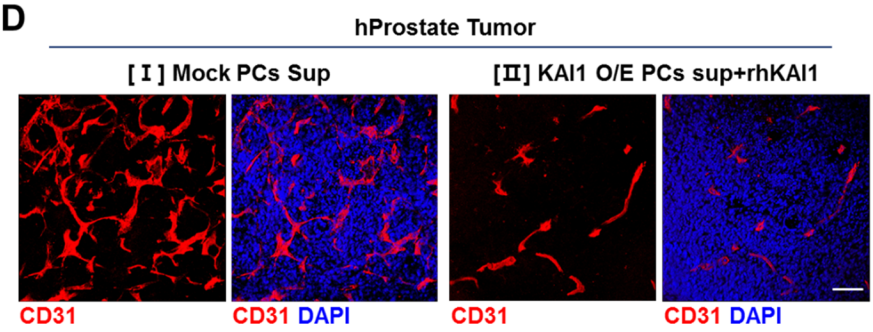

E

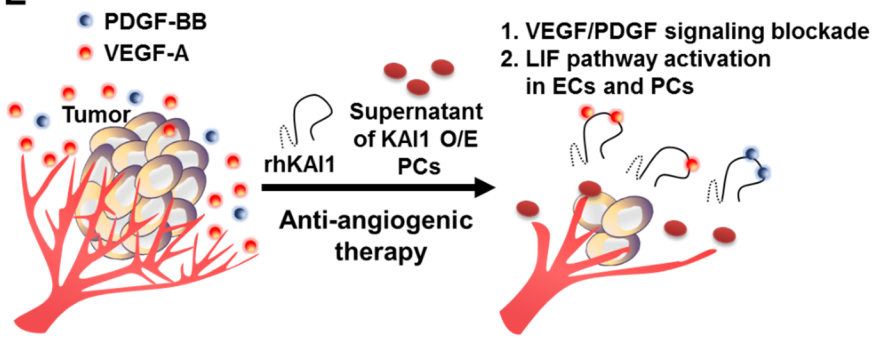

Figure 5. KAI1 expressed by pericytes and rhKAI1 protein showed therapeutic potential. (**A**) *In vitro* Matrigel tube formation assay using cellular spheroid consisting of MS1, 10T1/2, and B16 cells treated with 40 ng/mL of rhVEGF following the treatment with rhKAI1 (800 ng/mL). Scale bar, 100 μm. (**B**) B16 cells were subcutaneously injected in C57BL/6 mice with *Kai1*−O/E pericyte supernatant and rhKAI1 (**p<0.05, n=3). Scale bar, 5 mm. (**C**) PC3 cells were subcutaneously injected into NSG mice in combination with *Kai1*−O/E pericyte supernatant and rhKAI1(**p<0.05, n=7). Scale bar, 5 mm. (**D**) CD31 (red) immunostaining, and DAPI (blue) staining of human prostate (PC3) tumours treated according to *Kai1*−O/E pericyte supernatant and rhKAI1. Scale bar, 100 μm (**E**) Therapeutic potential of *Kai1*−O/E pericyte supernatant, for LIF induction, or rhKAI1, for VEGF quenching, in the treatment of cancer−related neo−angiogenesis and tumour growth.

DISCUSSION

KAI1 is the key molecule to control angiogenesis or to switch angiogenic milieu to quiescent one. When quiescent situation is required and induced, KAI1 that is palmitoylated by zDHHC4 and localized in the lipid raft membrane of pericytes induces transcription of LIF through Src/P53 axis, leading to turn-off of the angiogenic genes in pericytes (VEGF-A) as well as in ECs (Sox17, Angiopoietin2, and Esm1). Another anti-angiogenic mechanism of KAI1 is its binding to VEGF-A and PDGF-BB, leading to inhibition of phosphorylation or activation of VEGF-R2 or PDGF-R. Finally, we showed the therapeutic potential of KAI1 using in vivo cancer model by showing that tumour angiogenesis and growth can be suppressed by treatment with KAI1 (rhKAI and *Kai1*-O/E pericytes) **(Fig. 4F and 5E)**.

Generally, vascular ECs are dormant in human, but, following the activation of the angiogenic switch, these cells are induced to proliferation. This switch is turned off due to the equilibrium between the pro- and anti-angiogenic factors in tissues, but in the altered environments, such as cancer and wound-healing

environments, angiogenesis is activated. Even when VEGF is abundant in the microenvironment, EC proliferation and sprouting are not induced when KAI1 is overexpressed on pericytes, indicating that a decrease in KAI1 expression of pericytes represents an angiogenic switch, facilitating VEGF-induced angiogenesis, and it is essential for the initiation of angiogenesis.

Many issues remain to be elucidated regarding the mechanisms underlying the angiogenic switch involving KAI1, including the identification of KAI1-associated anti-angiogenic mechanisms, in addition to the VEGF/PDGF blocking ability and the induction of LIF secretion from pericytes. Furthermore, the possibility that KAI1 is contained in exosomes or secreted should be examined, together with the degree of KAI1 expression in tissue cells and its association with pro-angiogenic and anti-angiogenic microenvironments. Similarly, the effects of KAI1 decrease should be examined.

In this study, we used Blitz (ForteBio) to confirm the binding between KAI1 and cytokines, then we obtained the same result that KAI1 inhibited both VEGF and PDGF, not bFGF.

Interestingly, VEGF is known to be structurally very similar to PDGF, and recent reports have shown that PDGF can use VEGFR2, a receptor for VEGF, as a receptor[19].

Therefore, it is necessary to carry out a collaborative study between studies that reveal the common motif of VEGF and PDGF that bind to VEGFR2, and studies that reveal the sequence and structure of KAI1 molecule that plays a key role in anti-angiogenic role. If it is possible to identify peptide candidates from KAI1 sequences for anti-angiogenic that can inhibit VEGF and PDGF at the same time, it will be possible to advance the development of therapeutic agents for cancer or various vascular diseases.

Currently, the emerging concept for the anti-angiogenic cancer therapy is the normalization of tumour vasculature. One of the hallmarks of cancer vessels is that there are no or some loosely attached pericytes. Therefore, we postulate that the co-administration of conventional chemo- and radiation therapy together with the administration of KAI1-O/E pericytes may lead to the improvement of therapeutic effectiveness.

In conclusion, we identified a novel endogenous switch to turn angiogenesis off, KAI1 that is mainly expressed in pericytes and triggers quiescent milieu through induction of the pivotal anti-angiogenic LIF or through direct binding to and inhibition of VEGF and PDGF. The importance of pericytes as the controller of ECs in the context angiogenic equilibrium as well as provide a novel drug candidate for the treatment of various diseases associated with the altered angiogenesis. KAI1 expressed on pericytes or secreted may be useful diagnostic or prognostic biomarkers for cancer and other diseases.

REFERENCES

1 Potente, M., Gerhardt, H. & Carmeliet, P. Basic and therapeutic aspects of angiogenesis. *Cell* **146**, 873-887, doi:10.1016/j.cell.2011.08.039 (2011).

2 Liu, W. M. & Zhang, X. A. KAI1/CD82, a tumor metastasis suppressor. *Cancer Lett* **240**, 183-194, doi:10.1016/j.canlet.2005.08.018 (2006).

3 Hur, J. *et al.* CD82/KAI1 Maintains the Dormancy of Long-Term Hematopoietic Stem Cells through Interaction with DARC-Expressing Macrophages. *Cell stem cell* **18**, 508-521, doi:10.1016/j.stem.2016.01.013 (2016).

4 Alexander, M. S. *et al.* CD82 Is a Marker for Prospective Isolation of Human Muscle Satellite Cells and Is Linked to Muscular Dystrophies. *Cell stem cell* **19**, 800-807, doi:10.1016/j.stem.2016.08.006 (2016).

5 Nyberg, P., Xie, L. & Kalluri, R. Endogenous inhibitors of angiogenesis. *Cancer Res* **65**, 3967-3979, doi:10.1158/0008-5472.CAN-04-2427 (2005).

6 Bergers, G. & Benjamin, L. E. Tumorigenesis and the angiogenic switch. *Nat Rev Cancer* **3**, 401-410, doi:10.1038/nrc1093 (2003).

7 Kobayashi, M., Inoue, K., Warabi, E., Minami, T. & Kodama, T. A simple method of isolating mouse aortic endothelial cells. *Journal of atherosclerosis and thrombosis* **12**, 138-142 (2005).

8 Pitulescu, M. E., Schmidt, I., Benedito, R. & Adams, R. H. Inducible gene targeting in the neonatal vasculature and analysis of retinal angiogenesis in mice. *Nature protocols* **5**, 1518-1534, doi:10.1038/nprot.2010.113 (2010).

9 George, K. S., Wu, Q. & Wu, S. Effects of freezing and protein cross-linker on isolating membrane raft-associated proteins. *Biotechniques* **49**, 837-838, doi:10.2144/000113541 (2010).

10 Allen, J. A., Halverson-Tamboli, R. A. & Rasenick, M. M. Lipid raft microdomains and neurotransmitter signalling. *Nat Rev Neurosci* **8**, 128-140, doi:10.1038/nrn2059 (2007).

11 Zhou, B., Liu, L., Reddivari, M. & Zhang, X. A. The palmitoylation of metastasis suppressor KAI1/CD82 is important for its motility- and invasiveness-inhibitory activity. *Cancer Res* **64**, 7455-7463, doi:10.1158/0008-5472.CAN-04-1574 (2004).

12 Termini, C. M., Lidke, K. A. & Gillette, J. M. Tetraspanin CD82 Regulates the Spatiotemporal Dynamics of PKCalpha in Acute Myeloid Leukemia. *Sci Rep* **6**, 29859, doi:10.1038/srep29859 (2016).

13 Subramanian, A. *et al.* Gene set enrichment analysis: A knowledge-based approach for interpreting genome-wide expression profiles. *Proceedings of the National Academy of Sciences of the United States of America* **102**, 15545-15550, doi:10.1073/pnas.0506580102 (2005).

14 Kubota, Y., Hirashima, M., Kishi, K., Stewart, C. L. & Suda, T. Leukemia inhibitory factor regulates microvessel density by modulating oxygen-dependent VEGF expression in mice. *J Clin Invest* **118**, 2393-2403, doi:10.1172/JCI34882 (2008).

15 Lee, S. H. *et al.* Notch pathway targets proangiogenic regulator Sox17 to restrict angiogenesis. *Circ Res* **115**, 215-226, doi:10.1161/CIRCRESAHA.115.303142 (2014).

16 Goveia, J. *et al.* Endothelial cell differentiation by SOX17: promoting the tip cell or stalking its neighbor instead? *Circ Res* **115**, 205-207, doi:10.1161/CIRCRESAHA.114.304234 (2014).

17 Hu, W. W., Feng, Z. H., Teresky, A. K. & Levine, A. J. p53 regulates maternal reproduction through LIF. *Nature* **450**, 721-U728, doi:10.1038/nature05993 (2007).

18 Nomura, S. *et al.* Inhibition of VEGF-dependent angiogenesis by the anti-CD82 monoclonal antibody 4F9 through regulation of lipid raft microdomains. *Biochemical and biophysical research communications* **474**, 111-117, doi:10.1016/j.bbrc.2016.04.081 (2016).

19 Mamer, S. B. *et al.* Discovery of High-Affinity PDGF-VEGFR Interactions: Redefining RTK Dynamics. *Sci Rep* **7**, 16439, doi:10.1038/s41598-017-16610-z (2017).

국문 초록

혈관신생은 새로운 혈관을 생성하는 것으로 다양한 인자에 의해 조절된다. 대표적인 혈관신생 인자인 혈관내피세포성장인자(VEGF)가 있으며, 이를 억제하여 항암제로 사용할 수 있다. 하지만 이러한 체내 혈관내피세포성장인자 억제자들에 대해서는 잘 알려져 있지 않다. CD82/KAI1 이 혈관주변세포에서 발현되며, 혈관신생을 억제하는 것을 확인했다. *Kai1* 결핍 마우스는 혈관신생이 증가되 있다. 그 기전으로, KAI1 은 Src/p53 pathway 를 통해 LIF 의 발현/분비를 증가 시킨다. 또한 KAI1 은 혈관내피성장인자와 결합하여, 혈관내피세포의 VEGFR 신호전달을 억제하며, 튜브 형성을 억제한다. KAI1 과발현 혈관주변세포의 상등액 또는 KAI1 재조합 단백질은 암세포 환경에서 혈관을 억제하며, 암세포의 성장을 억제시킨다. 따라서, KAI1 은 혈관신생인자의 결합 및 항혈관신생인자의 분비 증가를 통해, 새로운 항암제 개발에 사용될 수 있다.

주요어: KAI1, 혈관신생, 내재적 혈관내피성장인자 억제자, 주피세포

학번: 2013-23535